J. Nano- Electron. Phys.
3 (2011) No1, P. 323-329

PACS numbers: 73.21. – b, 73.22. – f

CORRELATION OF RAMAN AND PHOTOLUMINESCENCE SPECTRA OF Al_2O_3 CAPPED SILICON NANOPARTICLES GROWN BY REACTIVE PULSED LASER DEPOSITION

***A.P. Detty*[1,2], *L.M. Kukreja*[1], *B.N. Singh*[1], *V.G. Sathe*[3], *T. Shripathi*[3], *V.P. Mahadevan Pillai*[2]**

[1] Laser Materials Processing Division,
Raja Ramanna Centre for Advanced Technology,
Indore, 452013, Madhya Pradesh, India

[2] Department of Optoelectronics, University of Kerala,
Karyavattom, 695581, Thiruvananthapuram, Kerala, India
E-mail: dettyalappatt@gmail.com

[3] UGC-DAE Consortium for Scientific Research,
Khandwa Road, 452 017, Indore, Madhya Pradesh, India

Synthesis and observation of a correlation between the Raman spectra and photoluminescence (PL) of silicon nanoparticles (Si-nps) embedded in Al_2O_3 matrix grown by reactive pulsed laser deposition in oxygen atmosphere are reported. We observed a strong dependence of the band gap, photoluminescence intensity and Raman spectra of Si-nps on the ambient oxygen gas pressure during the deposition. It appears that with increasing oxygen pressure the enhanced oxidation of silicon into SiO_x, which surrounds the Si-nps is responsible for the increase in the band gap, enhancement in the PL intensity and suppression of the Si related Raman mode observed in these studies.

Keywords: *SILICON NANOPARTICLES, REACTIVE PULSED LASER DEPOSITION, PHOTOLUMINESCENCE, MICRO-RAMAN SPECTRA, INTERFACE ENERGY STATES.*

(Received 04 February 2011, in final form 03 May 2011)

1. INTRODUCTION

Silicon (Si) is the mainstay material in the electronics industry since 1950's. However, the role of Si in photonics is limited due to poor optical performance of bulk Si because of its indirect band structure [1]. The discovery of room temperature luminescence from nanostructured Si [2, 3] reverted this notion and brought out prospects for its new applications including laser diodes and photodetectors in the emerging field of optoelectronics. In the past two decades, much effort has been devoted towards developing highly efficient luminescent silicon nanostructures. This include porous Si [2], silicon nanowires [4], silicon quantum dots [5], Si nanoparticles (Si-nps) embedded in suitable wide band gap materials [6], hydrogenated nanocrystalline silicon thin films [7], Si/SiO_2 superlattices [8] and quantum wells [9]. Among them silicon nanoparticles embedded in alumina (Al_2O_3) matrix exhibit interesting optical properties. Alumina serves as a good passive medium for the isolation of Si-nps because of its

excellent insulating, dielectric and thermal properties. Moreover, its high band gap of about 9.9 eV (in the form of sapphire) allows one to probe the optical properties of the embedded Si-nps even in the ultra violet (UV) region without any interference from the intervening medium [10].

Among the available deposition methods, pulsed laser deposition (PLD) is a suitable technique to grow Si-nps with desired particle size and size distribution in multilayer fashion with proper capping and considerable number density of the nanoparticles [11]. Moreover, PLD is a simple and versatile technique for growing stoichiometric, high-quality nanoparticles in inert and reactive ambient gases [12, 13]. Since oxygen is highly reactive, its use in ablation process of a Si target provides good control over the degree of oxidation and hence on the nanoparticles' size, by varying ambient pressure [14]. Fang et al. reported the synthesis of photoluminescent silicon nanocrystals using reactive PLD in oxygen atmosphere [6]. Uchida et al. prepared luminescent nanocrystalline silicon embedded in SiO_2 and Al-doped SiO_2 matrix in O_2 gas using laser ablation method [15]. The dependence of PL intensity on the ambient pressure of oxygen on PLD grown nanocrystalline silicon was reported by Riabinina et al. [16]. Recently, we reported photo-emission in the UV region from Si-nps embedded in Al_2O_3 matrix grown by PLD [17]. We report in this paper, to the best of our knowledge, for the first time a correlation between Raman and photoluminescence spectral features of Al_2O_3 capped multilayer ensembles of Si-nps grown by reactive PLD.

2. EXPERIMENTAL METHODS

2.1 Growth of multilayer ensembles of alumina capped Si-nps using reactive PLD

The third harmonic from a Quantel make Q-switched Nd:YAG laser (355 nm, 6 ns and 10 Hz) with a fluence of about 1.6 J/cm^2 was used to ablate the targets kept in a vacuum chamber. Initially, the chamber was evacuated down to a base pressure of ~ 5×10^{-6} mbar using a turbo molecular pump. During deposition high purity oxygen gas at constant pressure was admitted into the chamber through a control valve. The multi target assembly consisted of single crystalline silicon wafer (1×1 cm^2) and sintered alumina pellet. High purity Al_2O_3 powder was compacted and sintered at 1400 °C for 2 h, to make Al_2O_3 pellet of diameter of ~ 2 cm. The depositions of Si-nps were carried out on properly cleaned single crystalline sapphire substrates at a temperature of ~ 600 °C. The substrates were fixed at a distance of 5 cm from the targets. To ensure uniform ablation, the targets were rotated continuously during the deposition.

Initially, a base layer of alumina was deposited for 120 s on the sapphire substrates. Following those 20-layer structures of Si-nps and alumina capping layer were grown by the alternate ablation of the respective targets. In all the samples, the Si-nps and the capping layers were ablated for 60 and 120 s respectively. In this experiment isolated Si-nps were grown in high vacuum and in different partial pressures of ambient oxygen: p(O_2) varying from 5×10^{-4} to 1 mbar.

2.2 Characterization studies

The optical transmission spectra of Si-nps were recorded at room temperature (RT) using a UV-VIS spectrophotometer (Varian Cary 50) within the spectral range of 200-1000 nm. Labram-HR 800 spectrometer equipped with a Peltier cooled charge coupled device (CCD) detector was used to record the micro-Raman spectra of Si-nps in a back scattering geometry. The samples kept at RT were excited with the 488 nm line of an argon ion laser at 10 mW power. Spectra were acquired within an integration time of 120 s. A high-resolution 1800 grooves/mm grating was used for the Raman measurements, giving the spectral resolution of ~ 1 cm^{-1}. The photoluminescence studies were carried out using a CW He-Cd laser operating at 325 nm and 20 mW as an excitation source. During measurements the samples were kept at 16 K using a liquid He cooled cryostat. Although PL from these multilayer ensembles of Si-nps could also be observed at room temperature but the intensity was low and the spectral features were not well resolved. The temperature dependent PL spectral features from PLD grown Si-nps have been reported earlier by us elsewhere [17]. The valance states of Si in the nanoparticles were studied using X-ray photo-electron spectroscopy. This study revealed the degree of oxidation of the Si in the samples grown at different oxygen pressures in the reactive PLD.

3. RESULTS AND DISCUSSION

Figure 1a shows the transmission spectra of alumina capped multilayer ensembles of Si-nps grown in high vacuum and different partial pressures of oxygen. These spectra were acquired with reference to a thin film of Al_2O_3 deposited for 42 min keeping the other growth parameters as described in section 2.1. This was to subtract the possible spectral effects of the capping layers on the optical transmittance of Si-nps. All the samples grown in ambient oxygen are highly transparent in the visible region with average transmission ranging from 79 to 82 %, whereas the sample grown in vacuum showed lower transmission (average transmission ~ 53 %). In reactive depositions at high oxygen partial pressures, the amount of material deposited will be less due to increased collisions of plume constituents with gas molecules and scattering of ablated species [12]. In particular, at very high pressures of background gas, significant collision resistance to the plume causes a significant reduction in the deposition rate [18]. Due to this, the multilayer ensemble of Si-nps grown in high oxygen pressures may render less effective optical thickness to the incident radiation compared to those grown in vacuum. This in turn may lead to a decrease in optical absorption of these Si-nps. Significant increase in optical transmittance with ambient oxygen pressure can also be attributed to the higher degree of oxidation of Si-nps. Similar results were reported by Sullivan et al. in air annealed amorphous Si/SiO_2 superlattices grown by magnetron sputtering [19].

The dependence of optical band gap of as-grown Si-nps estimated from these absorption spectra using the standard tangent method on the partial pressure of oxygen is shown in Figure 1b. As can be seen in this figure, the band gap energy of Si-nps increases with an increase in background oxygen pressure up to 5×10^{-2} mbar. At pressures beyond 5×10^{-2} mbar, the band gap seems to have large fluctuations. Nevertheless, in all samples the absorption threshold

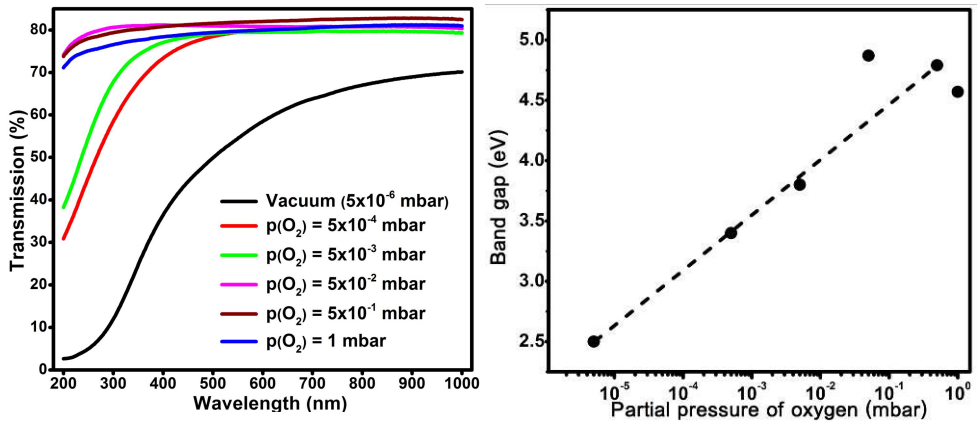

a b

Fig. 1 *– Room temperature transmission spectra of the PLD grown multilayer ensembles of Si-nps (a) and variation of the band gap with partial pressure of oxygen; dashed line is a visual fit (b)*

of Si-nps is well above the bulk Si band gap (~ 1.17 eV) and shifts to shorter wavelengths with increasing oxygen pressure during the PLD. At higher oxygen pressures, the plume species reaching the substrate are expected to have much reduced velocities due to the collision resistance effects of the background gas [18]. Thus, only comparatively smaller sized particles may gain enough momentum to diffuse through the ambient to reach the substrate. Hence a decrease in the particles size of Si-nps is expected with an increase in partial pressure of oxygen. Thus the observed blue shift in the optical band edge with oxygen pressure may be due to the widening of indirect band gap of Si-nps as a result of quantum confinement effect [20]. Another possible mechanism for the observed blue shift of optical band gap may be the formation of Si/SiO_x composites due the oxidation of the ablated Si species within the plume. At higher oxygen pressures, saturation of dangling bonds might produce thicker oxide shell over the Si-nps core. Optical transitions may occur within the much wider oxide band gap.

Figure 2 depicts the evolution of micro-Raman spectra of Si-nps with ambient oxygen pressure. It is well known that Raman scattering is highly sensitive to the chemical nature of the material, crystalline quality and size of the nanoparticles. The broad band centered at ~ 480 cm^{-1} is a characteristic of the transverse optical (TO) mode of Si-nps, which arises due to an enhanced disorder in the Si–Si network [21, 22]. This peak is prominent in the high vacuum grown sample and the peak intensity is found to be dependent on the background oxygen pressure. The peak almost vanished in samples grown at higher oxygen pressures. This is an indication of complete oxidation of Si-nps at higher pressures of background oxygen [23]. A weak shoulder ~ 308 cm^{-1} observed in high vacuum grown sample is also ascribed to the combination of the disorder induced LA and LO modes of amorphous Si–Si bond [24]. The sharp peaks observed at ~ 377, 418, 430, 448, 576 and 751 cm^{-1} are assigned to various optical and acoustic modes of Al_2O_3 capping layer [25].

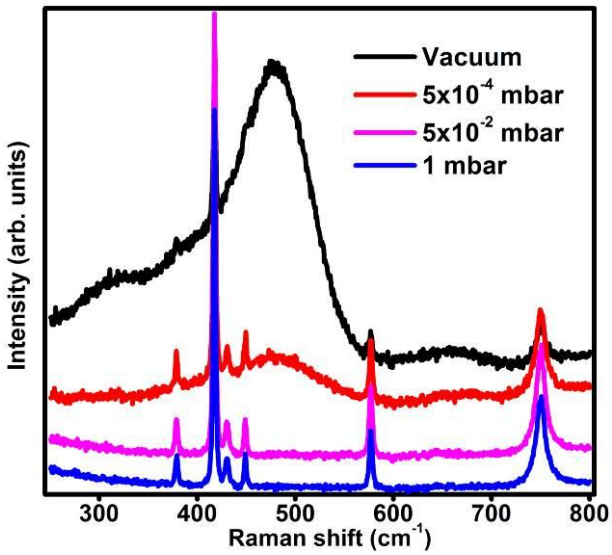

Fig. 2 – *Micro-Raman spectra of Si-nps embedded in Al_2O_3 matrix at different background oxygen pressure*

An intense PL in UV spectral region was observed at low temperature (16 K) from multilayer ensembles of alumina capped Si-nps. As shown in Figure 3a, the intensity of this peak at ~ 3.367 eV (369 nm) increased significantly upon introducing oxygen gas. A direct correlation between Raman and PL peak intensity variation with oxygen partial pressure can be seen from Figures 2 and 3a. This implies that as we increase the oxygen pressure the disordered state of Si-nps increases due to the formation of SiO_x. Thus one may infer that the PL signal might be originating from the Si/SiO_x energy states [26].

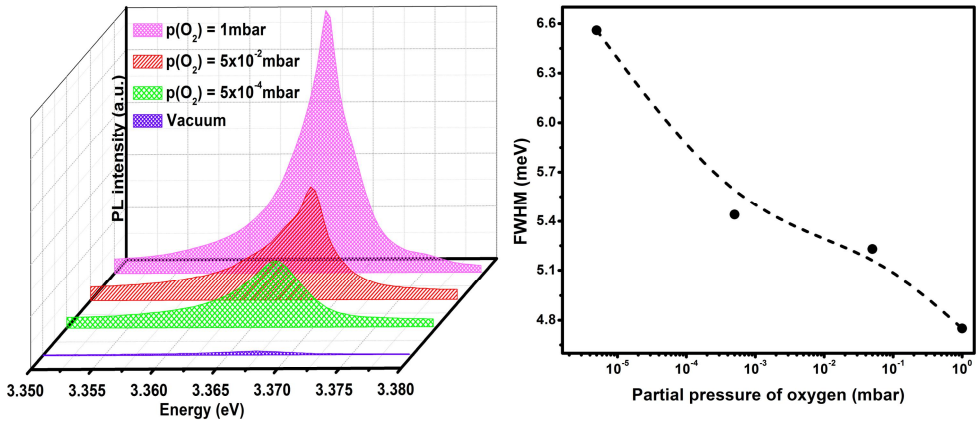

a b

Fig. 3 – *Low temperature PL spectra of alumina capped Si-nps grown in different background oxygen pressure (a) and variation of FWHM of the PL peaks with partial pressure of oxygen during the growth of the Si-nps (b)*

The dependence of FWHM of this peak with oxygen pressure is shown in Figure 3b. The emission line width shows a continuous narrowing with increase in background oxygen pressures. Comparatively narrow line width as sharp as 4.75 meV was obtained for sample grown at 1 mbar oxygen pressure. The reason for this dependence of the FWHM with oxygen pressure is not very clear at the moment and is a subject of our ongoing studies on this system.

To confirm the oxidation states of Si in the nanoparticles we carried out X-ray photo-electron spectroscopy (XPES) measurements on the samples grown at different pressures of oxygen ambient during the reactive PLD. The XPES data at different oxygen pressures are shown in Figure 4. The experimentally obtained peaks were deconvoluted, which are also shown in Figure 4. The XPES peak at 99.7 eV corresponds to the unbound Si and the peaks in the region of 100.5 – 103.5 eV correspond to the different valance states of Si bound to oxygen [27]. It can be clearly seen in this figure that as the ambient oxygen pressure is increased the relative fraction of unbound Si is decreasing and those of different valance states of Si bound to oxygen is increasing. This confirms our line of thought that with increasing oxygen ambient pressure more density of the Si/SiO_x states are formed.

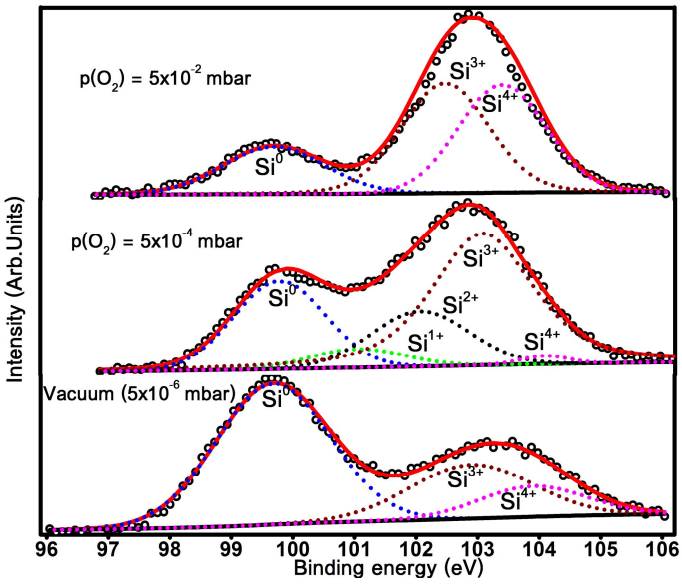

Fig. 4 *– X-ray photo-electron spectra of Si nanoparticles grown at different pressures of oxygen ambient during the reactive pulsed laser deposition*

In conclusion, we have grown luminescent Si-nps using reactive PLD in high vacuum and at different ambient oxygen pressures. A blue shift in the optical band gap with oxygen pressure in the transmission spectrum of these nanoparticles is observed. A strong correlation exists between the variation of Raman and PL peak intensities with ambient oxygen pressure. This reveals a highly disordered nature of the Si/SiO_x system grown at high oxygen pressures due to enhanced oxidation of Si. Thus the observed UV PL

emission could be originating from the transitions from the luminescence centers at the interface between Si-nps and the SiO_x surrounding layers.

REFERENCES

1. S.S. Iyer, Y.-H. Xie, *Science* **260**, 40 (1993).
2. L.T. Canham, *Appl. Phys. Lett.* **57**, 1046 (1990).
3. H. Takagi, H. Ogawa, Y. Yamazaki, A. Ishizaki, T. Nakagiri, *Appl. Phys. Lett.* **56**, 2379 (1990).
4. S.M. King, S. Chaure, S. Krishnamurthy, W.J. Blau, A. Colli, A.C. Ferrari, *J. Nanosci. Nanotechno.* **8**, 4202 (2008).
5. I. Sychugov, R. Juhasz, J. Valenta, M. Zhang, P. Pirouz, J. Linnros, *Appl. Sur. Sci.* **252**, 5249 (2006).
6. F. Fang, W. Zhang, J. Sun, N. Xu, J. Zhu, Z. Ying, J. Wu, *J. Mater. Res.* **24**, 2259 (2009).
7. W. Wei, G. Xu, J. Wang, T. Wang, *Vacuum* **81**, 656 (2007).
8. A.N. Rudenko, V.G. Mazurenko, *Phys. Solid State* **52**, 2409 (2010).
9. Z.H. Lu, D. Grozea, *Appl. Phys. Lett.* **80**, 255 (2002).
10. Q. Wan, N.L. Zhang, X.Y. Xie, T.H. Wang, C.L. Lin, *Appl. Sur. Sci.* **191**, 171 (2002).
11. R. Ciach, J. Morgiel, W. Maziarz, E.G. Manoilov, E.B. Kaganovich, S.V. Svechnikov, E.M. Sheregii, *Thin Solid Films* **318**, 154 (1998).
12. L.M. Kukreja, B.N. Singh, P. Misra, *Bottom-Up Nanofabrication: Supramolecules, Self-Assemblies and Organized Films*, (California: American Scientific: 2009).
13. D.H. Lowndes, D.B. Geohegan, A.A. Puretzky, D.P. Norton, C.M. Rouleau, *Science* **273**, 898 (1996).
14. D. Riabinina, C. Durand, J. Margot, M. Chaker, G.A. Botton, F. Rosei, *Phys. Rev. B* **74**, 075334 (2006).
15. N. Uchida, T. Okami, H. Tagami, N. Fukata, M. Mitome, Y. Bando, K. Murakami, *Physica E* **38**, 31 (2007).
16. D. Riabinina, C. Durand, M. Chaker, F. Rosei, *Appl. Phys. Lett.* **88**, 073105 (2006).
17. L.M. Kukreja, A. Chaturvedi, B.N. Singh, A.P. Detty, V.P.M. Pillai, J. Sartor, H. Kalt, C. Klingshirn, *Int. J. Nanosci.* (in press).
18. S. Amoruso, C. Aruta, R. Bruzzese, D. Maccariello, L. Maritato, F. M. Granozio, P. Orgiani, U.S. di Uccio, X. Wang, *J. Appl. Phys.* **108**, 043302 (2010).
19. B.T. Sullivan, D.J. Lockwood, H.J. Labbe, Z.-H. Lu, *Appl. Phys. Lett.* **69**, 3149 (1996).
20. W.L. Wilson, P.F. Szajowski, L.E. Brus, *Science*, **262**, 1242 (1993).
21. S. Hernandez, A. Martinez, P. Pellegrino, Y. Lebour, B. Garrido, E. Jordana, J.M. Fedeli, *J. Appl. Phys.* **104**, 044304 (2008).
22. Y.Q. Wang, Y.G. Wang, L. Cao, Z.X. Cao, *Appl. Phys. Lett.* **83**, 3474 (2003).
23. A.R. Wilkinson, R.G. Elliman, *J. Appl. Phys.* **96**, 4018 (2004).
24. G. Viera, S. Huet and L. Boufendi, *J. Appl. Phys.* **90**, 4175 (2001).
25. A. Misra, H.D. Bist, M.S. Navati, R.K. Thareja, J. Narayan, *Mater. Sci. Eng. B* **79**, 49 (2001).
26. H.Z. Song, X.M. Bao, N.S. Li, X.L. Wu, *Appl. Phys. Lett.* **72**, 356 (1998).
27. F. Iacona, S. Lombardo, S.U. Campisano, *J. Vac. Sci. Technol. B* **14**, 2693 (1995).